PRIFYSGOL
BANGOR
UNIVERSITY

Bedrock modulates the elevational patterns of soil microbial communities

He, Xianjin; Wang, Ruiqi; S. Goll, Daniel; Augusto, Laurent; Nunan, Naoise; Ellwood, M. D. F. ; Gao, Quanzhou; Huang, Junlong; Qian, Shenhua; Zhang, Yonghua; Shu, Zufei; Li, Buhang; Chu, Chengjin

Geoderma

Peer reviewed version

Cyswllt i'r cyhoeddiad / Link to publication

Bedrock modulates the elevational patterns of soil microbial communities

Xianjin He[1,2,*], Ruiqi Wang[1,*], Daniel S. Goll[2], Laurent Augusto[3], Naoise Nunan[4,5], M. D. Farnon Ellwood[6], Quanzhou Gao[7], Junlong Huang[8], Shenhua Qian[8], Yonghua Zhang[9], Zufei Shu[10], Buhang Li[1], Chengjin Chu[1,#]

1 State Key Laboratory of Biocontrol, School of Ecology, Shenzhen Campus of Sun Yat-sen University, Shenzhen, 518033, China.

2 Laboratoire des Sciences du Climat et de l'Environnement, IPSL-LSCE, CEA/CNRS/UVSQ, Orme des Merisiers, 91191, Gif sur Yvette, France.

3 ISPA, Bordeaux Sciences Agro, INRAE, 33140, Villenave d'Ornon, France.

4 Institute of Ecology and Environmental Sciences – Paris, Sorbonne Université, CNRS, IRD, INRAE, P7, UPEC, 4 place Jussieu, 75005 Paris, France.

5 Department of Soil and Environment, Swedish University of Agricultural Sciences, 75007 Uppsala, Sweden.

6 School of Environmental and Natural Sciences, Bangor University, Bangor, Gwynedd, LL57 2DG, United Kingdom.

7 Key Laboratory of Urbanization and Geosimulation of Guangdong Province, School of Geography and Planning, Sun Yat-sen University, Guangzhou, 510006, China.

8 Key Laboratory of the Three Gorges Reservoir Region's Eco-Environment, Ministry of Education, Chongqing University, Chongqing, 400045, China.

9 College of Life and Environmental Science, Wenzhou University, Wenzhou, 325035, China.

10 Guangdong Chebaling National Nature Reserve Administration Bureau, Shaoguan, China.

* These authors contributed equally to this work.

#Correspondence to Chengjin Chu: chuchjin@mail.sysu.edu.cn.

Acknowledgements

34

Abstract

36 Elevational gradients are often used to reveal how soil microorganisms will respond to climate

37 change. However, inconsistent microbial distribution patterns across different elevational

38 transects have raised doubts about their practical applicability. We hypothesized that variations

39 in bedrock, which influence soil physical and chemical properties, would explain these

40 inconsistencies. We therefore investigated soil microbial communities (bacterial and fungal)

41 along two adjacent elevational transects with different bedrocks (granite vs. slate) in a

42 subtropical forest. Our findings reveal that soil microbial communities are shaped by complex

43 interactions between bedrock type and environmental factors along elevational gradients.

44 Bacterial biomass was higher on slate, whereas fungal biomass was higher on granite. On

45 granite, both bacterial and fungal biomass increased with elevation, whereas divergent patterns

46 were observed on slate, likely due to the distinct soil properties or combinations of properties

47 influencing microbial biomass on each bedrock. Bedrock and elevation strongly influenced

48 microbial beta-diversity, with beta-diversity on granite driven primarily by soil total phosphorus

49 and moisture, and on slate by soil organic carbon and pH. In contrast, alpha-diversity was

50 impacted less by bedrock and elevation, but its relationship with environmental factors varied

51 markedly between bedrock types. Overall, our results highlight the critical influence of bedrock

52 in determining soil microbial community structure along elevational gradients and their potential

53 responses to climate change.

54

56

1. Introduction

58 As a proxy for the impacts of climate change on microbial communities, elevational

59 gradients provide unique insights into the regulatory mechanisms governing the spatial

60 distribution of soil microorganisms (Sundqvist et al., 2013). Studying the distributions of soil

61 microorganisms along elevational gradients not only reveals the mechanisms structuring soil

62   microbial communities (Nottingham et al., 2018; Peters et al., 2019), it also useful for

63   understanding the impacts of climate change on soil biogeochemical cycles (Bahram et al.,

64   2018; Hartmann and Six, 2022; Philippot et al., 2023). Numerous studies of the elevational

65   patterns of soil microbial communities have emerged over the past two decades (Bryant et al.,

66   2008; Fierer et al., 2011; He et al., 2020; Hendershot et al., 2017). However, these studies have

67   not found consistent trends in microbial biomass or community α-diversity: linear increases,

68   linear decreases, unimodal and concave trends have all been detected (He et al., 2020;

69   Hendershot et al., 2017; Wang et al., 2024). Environmental explanations for these disparate

70   patterns include climatic regions (He et al., 2020), vegetation types (Li et al., 2016), or

71   microclimate variation (Ma et al., 2022). However, the type of soil parent material -known as

72   "bedrock"- may also explain complex elevational patterns.

73   Spatial variations in soil microbial communities are influenced strongly by soil properties

74   (Fierer et al., 2009; Ni et al., 2022; Seaton et al., 2020). The factors shaping these communities

75   are often determined by specific combinations of local soil characteristics. For example, soil pH

76   is a well-established driver of bacterial community composition, particularly in acidic soils

77   (Griffiths et al., 2011; Tripathi et al., 2018). Similarly, the availability of nutrients such as nitrogen

78   and phosphorus plays a key role in regulating microbial dynamics, especially in nutrient-limited

79   ecosystems (Delgado-Baquerizo et al., 2017). While climatic factors along elevational gradients

80   tend to follow predictable trends within similar climate zones, the responses of soil microbial

81   communities to climate change may vary depending on underlying soil conditions (e.g., acidic

82   vs. neutral soils; nutrient-limited vs. nutrient-rich environments). Bedrock, as the parent material

83   for soil formation, influences a wide range of soil physico-chemical properties, including pH,

84   texture, and P levels (Augusto et al., 2017; He et al., 2021; Porder and Ramachandran, 2013;

85   Spinola et al., 2022; Zeng et al., 2023). Consequently, soil microbial communities on different

86   bedrock types may exhibit distinct responses to climate changes along elevational gradients,

87   reflecting the unique soil environments created by bedrock characteristics. In the present study,

88   we explored the extent to which bedrock can explain complex elevational patterns.

89   Bedrock varies in mountainous regions at both regional and local scales (Antonelli et al.,

90   2018), affecting the spatial patterns of soil microorganisms (He et al., 2024; Hu et al., 2020; Li et

91   al., 2018). However, only two studies have revealed that differences in bedrocks can affect the

92   response of soil microbes to elevational gradients (Bhople et al., 2019; Singh et al., 2014).

93   Singh et al. (2014) established two adjacent elevational transects on Mount Hana in South

94   Korea, one on basalt and one on coarse-grained basalt. They observed a triple-curve in

95 bacterial species richness on the basalt and a concave pattern on the coarse-grained basalt.

96 Bhople et al. (2019) showed a linear increase in soil microbial biomass on basaltic bedrock and

97 acidic soils, and a unimodal pattern on limestone bedrock with pH neutral soils.

98 Studies focusing on the influence of bedrock on elevational patterns of soil microbes are

99 remarkably scarce, and these studies often concentrate on a single feature of soil microbial

100 communities, such as biomass, or community α-diversity. Biomass, α-diversity, and β-diversity

101 are crucial characteristics of soil microbial communities, usually regulated by different factors.

102 Soil microbes are often carbon (C) limited, which is why microbial biomass is predominantly

103 driven by the availability of labile C (He et al., 2020). α-diversity is more responsive to variations

104 in soil pH (Fierer, 2017; Looby and Martin, 2020), particularly within acidic environments

105 (Calderón-Sanou et al., 2022). The β-diversity of soil microbial communities, which describes

106 the compositional variation among microbial communities across different environments, is

107 influenced by a complex interplay of factors (Chen and Lewis, 2023). With such diverse

108 characteristics of microbial communities being regulated by an assortment of environmental

109 factors, it is no surprise that the interactions between bedrock, elevation, and soil microbial

110 communities are extremely intricate.

111 In accordance with our hypothesis that bedrock modulates the environmental factors

112 regulating soil microbial communities at different elevations, we anticipate significant differences

113 in microbial community composition between the two bedrock types. Specifically, we expect to

114 find that: (1) Soil microbial biomass, α-diversity, and β-diversity differ between bedrock types.

115 We expect microbial biomass and α-diversity to increase on the slate transect due to its higher

116 SOC, phosphorus levels, and pH (He et al., 2021). (2) Bedrock type will govern the relationship

117 between elevation, microbial biomass and α-diversity. Given that key environmental conditions

118 structuring microbial communities differ on different bedrocks, we also predict that (3) factors

119 driving β-diversity along the elevational gradient will vary between the two bedrocks, and similar

120 environmental conditions may shape microbial community patterns differently on different

121 bedrock types.

122

123 **2. Materials and methods**

124 **2.1 Study sites**

125   We worked in the Chebaling National Nature Reserve in the Guangdong Province of
126 southern China (114°09′–114°16′E, 24°40′–24°46′N). The climate is a typical subtropical
127 monsoon (He et al., 2021). The geological structure of the Reserve belongs to the South China
128 fold system. Elevation ranges from 330 meters above sea level to 1,256 m.a.s.l. Cambrian and
129 Ordovician strata are present in the northwest section. Northeast-southwest slate was formed
130 after fold-fracture. The middle and south are Cambrian strata, forming slate mountains. The
131 northern parts experienced intrusion of Jurassic plutonic rocks, forming acid plutonic rock
132 mountains. Soils are classified in the Ultisol order and the Udult suborder based on the USDA
133 soil classification system (Zhou et al., 2013).

134   We identified two adjacent mountains with different bedrocks (granite and slate) in the
135 Chebaling National Nature Reserve (He et al. 2021). The geographic distance between the two
136 mountains does not exceed 10 km. The vegetation on both mountains is well-preserved
137 subtropical evergreen broad-leaved forest. The forest on the granite bedrock is dominated by
138 *Schima superba*, *Machilus chinensis,* and *Eurya nitida*, while the forest on the slate bedrock is
139 dominated by *Machilus chinensis, Eurya nitida* and *Rhododendron simsii*. A total of 18 sites
140 were established along two elevational transects (Fig. S1), with nine sites on each bedrock.
141 Plots were distributed at about 100-m intervals in elevation (determined by GPS) within each
142 transect, with elevations ranging from 410 to 1,080 m.a.s.l. on the granite bedrock and 350 to
143 1,120 m.a.s.l. on the slate bedrock. To reduce the influence of aspect, sampling plots were
144 located on the south side of any microtopography at each site.

145 2.2. Sampling and analytical methods

146   All plots (40 m x 40 m) were sampled in October 2018. All trees with a diameter at breast
147 height above 1 cm were recorded in each plot. We estimated the forest above-ground biomass
148 (AGB) using diameter at breast height of each tree and allometric relationships (Réjou-Méchain
149 et al., 2017). We installed a Micro Station Data Logger (USA, HOBO, H21-002) in each plot,
150 with two probes inserted into the soil (at a depth of approximately 10 cm) which monitored soil
151 temperature and moisture. Recordings were taken hourly from July 13, 2018, to July 13, 2019.
152 Here, we use the data collected over the entire year to calculate the soil mean annual
153 temperature (MAT) and moisture, which we use to explain the spatial variation of soil microbial
154 community characteristics.

155   Volumetric soil samples were taken to determine soil bulk density. Soil depth was more
156 than 100 cm in all but two of the high elevation sites in the slate transect. In these two plots, soil

157 depth was roughly 60 cm. These shallow soil depths were likely due to severe erosion on the

158 steeper slopes. Five subplots (10 × 10 m) were randomly selected at each site. We removed the

159 leaf litter from the forest floor and collected topsoil to a depth of 20 cm using a stainless soil

160 corer (inner diameter = 3.5 cm). We collected six random soil cores and homogenized them into

161 composite samples for each subplot. A total of 90 soil samples (i.e. 18 plots x 5 subplots) were

162 collected and transported on ice directly to the laboratory. Each soil sample was then passed

163 through a 2-mm sieve before being divided into two subsamples: one was stored at −80°C for

164 phospholipid fatty acid (PLFA) analysis and high-throughput sequencing (HTS), and one was

165 air-dried at room temperature for the measurement of soil physicochemical properties in the

166 laboratory.

167 We measured soil pH with a PHS-3C pH acidometer (soil-water ratio of 1:5) and used

168 dry combustion with an elemental analyser (Perkin Elmer 2400 Series II) to measure soil

169 organic carbon (SOC) and total N (TN) concentrations. Soil total P (TP) concentration was

170 measured using a nitric acid–perchloric acid digestion, followed by a colorimetric analysis

171 (Murphy and Riley, 1962) using a UV-Vis spectrophotometer (UV1800; Shimadzu, Kyoto,

172 Japan). We measured particle size distribution using a laser particle analyzer based on the laser

173 diffraction technique operating over a range of 0.02-2000 µm (Mastersizer 2000 particle size

174 analyzer, Malvern Instruments, Ltd., UK).

175 We used a modified PLFA analysis (Frostegård and Bååth, 1996) to determine bacterial

176 and fungal biomass. The abundance of individual fatty acids was expressed as µg per g of dry

177 soil. Concentrations of each PLFA were calculated based on the 19:0 internal standard

178 concentrations and microbial biomass was expressed as the sum of identifiable PLFAs. We

179 chose a set of fatty acids to represent bacterial PLFAs. Bacterial PLFAs were obtained by

180 summing the phospholipid fatty acid 14:00, 15:00, 16:00, 18:00, 13:0 anteiso, 13:0 iso, 14:0 iso,

181 14:1 ω5c, 15:0 anteiso, 15:0 iso, 15:1 ω6c, 16:0 iso, 16:1 ω5c, 16:1 ω7c, 17:0 anteiso, 17:0

182 cyclo ω7c, 17:0 iso, 18:1 ω7c, 18:1 ω9c, 19:0 cyclo ω7c, and 19:0 cyclo ω9c contents. Gram-

183 positive bacteria were identified by branched-chain fatty acids, including 13:0 anteiso, 13:0 iso,

184 14:0 iso, 15:0 anteiso, 15:0 iso, 16:0 iso, and 17:0 anteiso and iso. Gram-negative bacteria were

185 distinguished by monounsaturated and cyclopropyl fatty acids, specifically 14:1 ω5c, 15:1 ω6c,

186 16:1 ω5c, 16:1 ω7c, 17:0 cyclo ω7c, 18:1 ω7c, 18:1 ω9c, 19:0 cyclo ω7c, and 19:0 cyclo ω9c.

187 The sum of 18:2ω6c and 18:3 ω6c represented fungal PLFAs.

188   Soil DNA was extracted from composite soil samples using the FastDNA SPIN Kit for
189   Soil (MP Biomedicals, Heidelberg, Germany) and purified by agarose gel electrophoresis. The
190   quality of the DNA samples was checked on a spectrophotometer (NanoDrop, ND2000,
191   ThermoScientific, USA). Total DNA was used for high-throughput sequencing on an Illumina
192   MiSeq platform (San Diego, CA, USA). The bacterial V4 hypervariable region of the 16S rRNA
193   gene and fungal internal transcribed spacer (ITS) region was amplified using the primer pair
194   505F/816R (5′-GTGCCAGCMGCCGCGG-3′/5′-GGACTACHVGGGTWTCTA AT-3′) (Caporaso
195   et al., 2011) and ITS1F/ITS2 (5′-GGAAGTAAAAGTCGTAACAAGG-3′/5′-
196   GCTGCGTTCTTCATCGATGC-3′) (Shen et al., 2020) along with the Illumina adaptor sequence
197   and barcode sequences, respectively.

198   The raw sequence data were processed and analyzed using QIIME Pipeline (Caporaso
199   et al., 2011). To improve sequence quality we removed average quality (value ≤20) sequencing
200   reads with ambiguous nucleotides in barcodes, and homopolymer reads between 8 bp and 150
201   bp in length. Paired ends were joined with FLASH (Magoc and Salzberg, 2011). Chimeric
202   sequences were detected and eliminated using the Uchime algorithm (Edgar, 2013). All
203   sequences were clustered into operational taxonomic units (OTUs) at a 97% identity threshold.
204   Finally, the representative sequences of each OTU were classified against the RDP 16S rRNA
205   database for bacteria and UNITE Fungal ITS database for fungi with an 80% confidence
206   threshold. The resultant OTU abundance tables from these analyses were rarefied to an even
207   number of sequences per sample to ensure equal sampling depth (26,160 and 26,760 for 16S
208   rDNA and ITS, respectively). To minimize the influence of potentially spurious OTUs, we
209   excluded those with a total read count below 50 or present in fewer than five samples after
210   rarefaction. All subsequent analyses of α-and β-diversity were conducted based on this filtered
211   OTU table. The raw reads have been deposited into the National Centre for Biotechnology
212   Information (NCBI) Sequence Read Archive database (PRJNA1177672).

213   **2.3 Statistical analyses**

214   We used Wilcoxon tests to assess differences in microclimate, plant traits, and soil
215   properties between granite and slate bedrocks. To evaluate elevational trends, we applied
216   univariate linear regression models, while multivariate linear regression models were used to
217   examine soil microbial community responses across different elevations and bedrock types, as
218   well as to identify interactive effects. Model fit was evaluated using Akaike's Information
219   Criterion (AIC), with the model having the lowest AIC score selected as the best fit.

220   Spearman correlation analyses were conducted to determine whether bedrock type

221   influenced relationships between environmental variables and soil microbial communities.

222   Additionally, we applied multiple regression models to investigate associations between

223   microbial variables (bacterial and fungal biomass, biomass ratios, and alpha diversity indices)

224   and a range of environmental predictors, including soil properties, i.e., pH, moisture, clay

225   content, soil organic C (SOC), soil P, soil C-to-N ratio (C:N), soil C-to-P ratio (C:P), soil N-to-P

226   ratio (N:P), plant traits (above-ground biomass and plant Shannon diversity), and climatic

227   factors (mean annual temperature). Multicollinearity among predictors was assessed using

228   Variance Inflation Factor (VIF) values calculated with the *vif* function from the *car* package.

229   Initial VIF analysis revealed high collinearity among certain soil nutrient ratios (soil C:P and soil

230   N:P), with VIF values exceeding 100; thus, these variables were excluded, reducing the VIF of

231   all remaining predictors to below 5. To examine interactions between environmental predictors

232   and bedrock type, we incorporated selected interaction terms (bedrock:TP, bedrock:moisture,

233   bedrock:pH, and bedrock:MAT) aligned with our research questions. Due to the limited sample

234   size, we focused on these specific interactions rather than including all possible terms. Stepwise

235   model selection using AIC was performed with the *dredge* function from the *MuMIn* package to

236   identify best-fit models for each microbial variable, allowing for retention of the most informative

237   predictors while optimizing model performance.

238   We calculated the Chao1 index, Shannon, and Inverse Simpson diversity index as α-

239   diversity indices of soil microbial communities. Shannon index is defined as $H = -\sum_1^i P_i log P_i$,

240   where Pi is the proportional abundance of species i. Inverse Simpson index is defined as 1/D,

241   where $D = \Sigma P_i^2$. We used the Bray-Curtis-dissimilarities-based principal components analysis

242   (PCoA) to assess differences (β-diversity) in microbial communities in different sites and

243   bedrocks. We performed square root transformations of the OTU relative abundances before

244   the PCoA. We performed distance-based Redundancy Analysis (db-RDA) of the correlation

245   between predictor variables and microbial composition. We calculated these diversity indices

246   and conducted these ordination analyses using the *vegan* R package (Oksanen et al., 2020).

247   We performed a Principal Component Analysis (PCA) to visualize the variation in environmental

248   variables across elevational gradients on two bedrock types. The analysis was conducted using

249   the *PCA* function from the *FactoMineR* package. A biplot was created using *fviz_pca_biplot*

250   from the *factoextra* package. We used a neutral community model (NCM) (Sloan et al., 2006) to

251   test whether deterministic or stochastic processes were structuring the microbial communities.

252 We used *Hmisc*, *minpack.lm* and *stats4* packages for the NCM, with default parameters for
253 model fitting.

254   All statistical analyses were performed using R (R Core Team, 2023) and graphs were
255 generated with the ggplot2 package (Wickham, 2016).

256

257 3. Results

258 3.1 Effects of elevation and bedrock on soil characteristics

259   Wilcoxon tests showed no significant differences in soil MAT, moisture, and SOC
260 concentration between the granite and slate transects (Table S1). AGB, soil C:N, C:P, N:P
261 ratios, and soil silt and sand contents were higher on the granite transect, whereas plant
262 diversity, soil pH, bulk density, TN, TP, and clay content were lower on the granite than on the
263 slate transect. Univariate linear regression models revealed a consistent pattern of significant
264 declines in MAT, plant diversity and soil pH with elevation, and an increase in SOC, TN, TP and
265 silt content across both bedrock types (Fig. S2 and S3). Soil clay content and moisture showed
266 no significant elevational trend along either transect (Fig. S3). AGB decreased with elevation on
267 the granite but showed no significant trend on the slate (Fig. S2). PCA results revealed a clear
268 separation of sampling sites along PC1 (Figure S4). Key variables associated with PC1, such as
269 soil P, C:N, C:P, N:P, clay, and moisture, appear to be major environmental drivers of microbial
270 community differences between the two bedrocks. Variables closely aligned with PC2, including
271 elevation, MAT, SOC, and pH, are likely primary drivers of microbial community changes along
272 the elevational gradient within each transect.

273 3.2 Effects of elevation and bedrock on soil microbial biomass

274   Bacterial biomass was slightly higher on slate, whereas fungal biomass was higher on
275 granite (Table 1). Consequently, the bacteria-to-fungi biomass ratio (B/F) was significantly
276 higher on slate than on granite. Given that Gram-positive bacteria are ecologically and
277 functionally more similar to fungi, our findings align with this pattern: the Gram-positive to Gram-
278 negative bacteria ratio (G+/G- ratio) was significantly higher on granite than on slate. Notably,
279 both bacterial (B) and fungal (F) biomass, along with the G+/G- ratio increased significantly with
280 elevation on the granite but not on the slate transect; B/F ratios showed no significant linear
281 trends on either bedrock (Fig. 1). Multivariate linear regression models confirmed significant

282 impacts of elevation and bedrock on microbial biomass characteristics, including significant

283 interactive effects for bacterial and fungal biomass but not for B/F ratios or G+/G- ratios (Table

284 2).

285 The best models selected through stepwise regression provided strong explanatory

286 power for variations in microbial biomass, with adjusted R² values ranging from 0.45 to 0.71

287 (Table 3). Soil microbial biomass was shaped significantly by multiple environmental factors and

288 their interactions with bedrock type. For bacterial biomass, SOC, TP, and the soil C:N ratio were

289 key factors, with positive associations observed for soil C and P, and a negative association

290 with the C:N ratio. Fungal biomass was also influenced by SOC, C:N ratio, and TP, though the

291 impacts of moisture and MAT varied depending on bedrock type. The B/F biomass ratio was

292 shaped by soil moisture, plant Shannon diversity, and TP, with an interaction between moisture

293 and bedrock type. Additionally, the G+/G- ratio was driven by soil clay content, MAT, and pH,

294 with a significant interaction between TP and bedrock type.

295 Spearman correlations corroborated the multiple regression results (Tables S2 & S3).

296 On the granite transect, bacterial biomass was strongly associated with SOC and TP, whereas

297 on slate, no significant correlations were observed. Fungal biomass on granite correlated

298 positively with SOC and the soil N:P ratio, while being negatively associated with AGB and

299 MAT. On slate, fungal biomass correlated only with moisture. The B/F ratios on granite were

300 positively linked with soil TP and negatively to moisture, whereas on slate, they correlated

301 negatively with moisture. Additionally, the G+/G- ratios showed a strong positive correlation with

302 the soil N:P ratio on granite and a negative correlation with MAT on slate.

303 **3.3 Effects of elevation and bedrock on soil microbial community diversity and**

304 **composition**

305 Microbial richness, as indicated by Chao1 indices, was consistently and significantly

306 higher on slate for both bacterial and fungal communities (Table 1). In contrast, Shannon

307 indices showed no significant differences between bedrock types for either bacterial or fungal

308 communities, indicating comparable overall diversity. The inverse Simpson index, however, was

309 significantly lower for bacterial communities on slate than on granite, suggesting reduced

310 evenness and potential dominance by a few species on slate. Interestingly, soil microbial α-

311 diversity, encompassing Shannon and inverse Simpson indices, showed no clear elevational

312 trends (Fig. 2). Multivariate linear regression analyses confirmed these observations, identifying

313 significant differences between bedrock transects in the Chao1 and inverse Simpson indices for

314   bacteria, and in the Chao1 index for fungi, but not in other α-diversity measures. Additionally,

315   elevation significantly influenced only the fungal Chao1 index, with no observable effect on other

316   α-diversity indices or significant interactions between elevation and α-diversity (Table 2).

317   Regression models for diversity indices showed lower explanatory power compared with

318   biomass (adjusted R² = 0.20-0.38; Table 4). Bacterial Shannon index was significantly affected

319   by clay content, MAT, moisture, and pH, while the bacterial inverse Simpson index was

320   associated with soil C, P, and a moisture-bedrock interaction. Both the fungal Shannon and

321   inverse Simpson indices were influenced by soil P, soil C, and pH, with strong effects from

322   interactions between these variables and bedrock type; soil P, in particular, played a prominent

323   role in shaping fungal community diversity.

324   Spearman correlation analysis indicated that the Shannon index of the bacterial

325   community correlated positively with soil pH on both granite and slate transects (Table S2 and

326   S3). The inverse Simpson index of bacteria correlated positively with soil C:P and N:P ratios on

327   granite but showed no significant relationship on slate. The fungal community's Shannon index

328   correlated negatively with MAT on both bedrocks, and additionally with clay content on granite.

329   On slate, it correlated significantly with TP, C:P, and N:P. The inverse Simpson index for fungi

330   correlated negatively with clay on granite, whereas on slate it showed significant correlations

331   with soil pH, C:N, C:P, N:P, and other environmental factors (Table S3).

332   Principal Components Analysis results highlighted clear differences in beta-diversity,

333   i.e., the composition of soil microbial communities (bacterial and fungal), across different

334   bedrock types (Fig. 3 a & b). Results of db-RDA revealed that the compositions of soil bacterial

335   and fungal communities were determined primarily by the soil C:P and N:P ratios and TP

336   content (Fig. 3a). These findings indicate that variations in phosphorus level were key in driving

337   the differences in community composition observed between the bedrocks. Further db-RDA on

338   individual bedrock types revealed that on granite, soil TP content and moisture were crucial in

339   shaping both bacterial and fungal communities (Fig. 3 c & e). Conversely, on slate, SOC and

340   soil pH were the dominant factors influencing bacterial communities (Fig. 3d), whereas moisture

341   and clay content significantly affected fungal communities (Fig. 3f). This analysis suggests a

342   role for bedrock in mediating species turnover along elevational gradients, with changes in soil

343   P concentration and moisture levels being pivotal.

344   The fit of bacterial communities on granite to the NCM was higher (R^2 = 0.92; Nm =

345   18943) compared with slate (R^2 = 0.90; Nm = 16458) (Fig. S6 a & b), suggesting the importance

of stochastic processes in the assembly of these bacterial communities. In the case of the fungal communities, the fit to the NCM was comparable between granite (R^2 = 0.62; Nm = 1237) and slate (R^2 = 0.62; Nm = 1209) , indicating no discernible difference in community assembly processes (Fig. S6 c & d).

4. Discussion

This study reinforces findings by Bhople et al. (2019) and Singh et al. (2014), confirming that bedrock composition plays a critical role in shaping soil microbial community responses along elevational gradients in subtropical mountain ecosystems. While this and previous studies each focused on a single transect per bedrock type, together they provide robust evidence that bedrock type significantly influences microbial elevational patterns. Unique combinations and ranges of soil properties are established by different bedrock types, resulting in distinct microbial community distributions along elevation gradients. Moreover, the impact of specific environmental factors on microbial communities varies with bedrock type, highlighting the interactive effects between bedrock and environmental conditions on microbial distribution. These interactions deepen our understanding of the intricate dynamics of microbial communities and underscore the necessity to consider bedrock type when evaluating microbial responses to environmental changes.

4.1 Bedrock modulates the elevational patterns of soil microbial biomass

Bacterial and fungal biomass differed significantly on the contrasting bedrocks. Both transects were under similar climates, and we therefore conclude that differences in microbial biomass were likely caused by the variation of bedrock, which concurs with previous studies (Deng et al., 2015; Sun et al., 2016) (Deng et al., 2015; Sun et al., 2016). Deng et al. (2015), who worked in a similar subtropical monsoon climate, concluded that bedrock explained more variation in soil microbial biomass than land use, after discovering that microbial biomass in soil derived from granite was significantly higher than in soil derived from quaternary red earth and tertiary red sandstone. Sun et al. (2016) showed that agricultural soils derived from granite supported more microbial biomass than quaternary red clay soil and purple sandy shale, even after 40 years of agricultural use. These results further emphasize the fact that bedrock drives the spatial variation of soil microbial biomass.

376   Bacteria and fungi responded differently to the different bedrocks in our study, which is
377 further evidence of the regulatory effects of bedrock on microbial communities. Bacterial
378 biomass, particularly the amount of Gram-positive versus Gram-negative bacteria, was higher
379 on slate than on granite. This can be attributed to slate's higher soil TN and TP contents, closer-
380 to-neutral soil pH, and higher soil clay content, all of which favor bacterial growth. Bacteria,
381 especially Gram-positive types, rely heavily on nutrient availability (Yu et al., 2022), are more
382 sensitive to pH changes (Luan et al., 2023; Rousk et al., 2010), and benefit from the simplified
383 physical conditions of soils richer in clay (Philippot et al., 2023). In contrast, fungi are better at
384 extracting nutrients from decomposing organic matter (Koranda et al., 2014)q, and have a
385 greater tolerance to pH changes (Rousk et al., 2010). Moreover, their multicellular, filamentous
386 structure enables fungi to adapt to a variety of soil physical environments (Philippot et al., 2023).
387 Furthermore, considering the competitive dynamics between fungi and bacteria (Bahram et al.,
388 2018), the diminished bacterial biomass on granite reduces competition, potentially boosting
389 fungal biomass. These mechanisms clarify why fungal biomass was higher on granite than on
390 slate, providing insight into how bedrock variability distinctly influences bacterial and fungal
391 communities.

392   As well as observing the effects of the bedrock itself on soil microbial communities, we
393 also noticed inconsistencies in the elevational patterns of the soil microbial biomass along the
394 two transects. On the granite, soil bacterial and fungal biomass increased with elevation,
395 whereas on the slate, bacterial biomass showed no trend, and fungal biomass decreased
396 slightly. Soil microbes usually need to derive energy and nutrients from soil organic matter, and
397 as a result, their biomass is generally coupled with SOC concentration (He et al., 2020; Smith et
398 al., 2021). However, in this study, such a relationship was observed only on granite; on slate,
399 which had higher N and P levels, the biomass of bacteria and fungi did not show significant
400 correlations with SOC, soil TP content, MAT, or other factors. This may be attributed to the fact
401 that in nutrient-abundant environments, especially with sufficient P, soil microbes experience
402 lower nutrient limitations; and their reliance on the pathway of nutrient acquisition through the
403 decomposition of organic matter might be comparatively weaker (Lang et al., 2016). This would
404 certainly explain why microbial biomass was not correlated with SOC and TP concentrations on
405 slate. These findings suggest that the bedrock, by influencing the P levels in the soil and indeed
406 throughout the entire ecosystem, can impact the responses of soil microbial biomass to
407 elevational gradients.

408 **4.2 Bedrock modulates the elevational patterns of soil microbial community diversity**

13

409   The higher Chao1 index for both bacterial and fungal communities on slate than on
410   granite indicates greater microbial species richness in soils with higher nutrient content and pH
411   (Xiao et al., 2022). However, neither the Shannon nor the inverse Simpson index on slate were
412   significantly higher than on granite, suggesting that the increased richness on slate likely
413   reflects a greater presence of rare or low-abundance taxa, reducing overall community
414   evenness. In particular, the inverse Simpson index for bacterial communities was significantly
415   higher on granite than on slate. This may be attributed to the lower P, moisture, and pH levels
416   on granite, which may promote a broader range of microbial taxa that coexist more evenly.
417   Conversely, the higher P, moisture, and pH levels on slate could favor a few dominant species,
418   resulting in lower evenness despite the elevated species richness. Interestingly, unlike microbial
419   biomass, neither bacterial nor fungal α-diversity varied significantly with elevation on either
420   bedrock type, suggesting that soil microbial biomass and community α-diversity are regulated by
421   different factors (Li et al., 2020; Ren et al., 2018). These distinct responses between microbial
422   biomass and α-diversity, with their implications for ecosystem functioning, warrant further
423   exploration.

424   With regard to those factors influencing α-diversity, our multiple linear models explained
425   significantly less of the variation in α-diversity than in microbial biomass along the elevational
426   gradient. Alongside the high explanatory power of neutral community models (NCM) on both
427   bedrocks—especially with over 90% for bacterial communities—our findings suggest that
428   microbial community assembly along the elevation gradient was driven largely by stochastic
429   processes, with environmental factors playing a lesser role. While we found significant
430   relationships between soil pH and the Shannon indices for both bacteria and fungi, supporting
431   the notion that microbial α-diversity is sensitive to soil acidity (Luan et al., 2023; Smith et al.,
432   2021), α-diversity itself did not vary significantly with elevation. This is likely due to the relatively
433   small pH fluctuations across the transects. Despite the limited explanatory power of our models,
434   we observed that certain factors, such as soil phosphorus and moisture, had bedrock-specific
435   effects on microbial α-diversity. These significant interactions indicate that although α-diversity
436   did not shift noticeably with elevation, its relationship with environmental factors was still
437   modulated by bedrock.

438   Our findings suggest that bedrock impacts the β-diversity of soil microbial communities.
439   Bacteria and fungi displayed markedly distinct compositions across the two bedrocks. Our
440   observation that bedrock influences the composition of soil microbial communities aligns with
441   the conclusions of previous studies (Sheng et al., 2023; Tytgat et al., 2016; Weemstra et al.,

442 2020; Xiao et al., 2022). Studies of different bedrocks have proposed different mechanisms for

443 structuring soil microbial communities. For example, Tytgat et al. (2016) found that SOC content

444 structured bacterial communities, whereas Sheng et al. (2023) concluded that soil pH structured

445 the bacterial community composition among different bedrocks. We identified differences in soil

446 P as the primary mechanism structuring soil microbial communities on the granite and slate

447 bedrocks. On granite, soil TP content and moisture govern species turnover of both bacteria

448 and fungi, which is supported by another study in nearby subtropical forest (Chen and Lewis,

449 2023). On slate, however, the influence of soil P on species turnover appeared to be minimal.

450 This could be due to P not being a limiting factor, as slate and its associated soils have high P

451 concentrations. Together, these results indicate that bedrock type not only influences the

452 composition of soil microbial communities, but also modulates the primary drivers of microbial

453 community structure along elevational gradients.

454   Our results should be interpreted in light of the fact that our study was based on one

455 elevational transect per bedrock type. Nonetheless, given the inconsistency of previous studies

456 of soil microbial elevational patterns, including those based on single transects (e.g.,

457 Bayranvand et al., 2021; Peters et al., 2016; Zakavi et al., 2022), our findings provide relevant

458 and valuable insights into how bedrock influences microbial community patterns along elevation

459 gradients. Ideally, future studies should integrate multiple transects replicated within bedrock

460 types to more thoroughly understand the responses of soil microbial communities to climate

461 gradients.

462

5. Conclusion

463 **5. Conclusion**

464   We have shown that bedrock significantly influences soil microbial biomass and β-

465 diversity, while having limited effects on α-diversity. Moreover, bedrock modulated the impacts

466 of the elevation gradient on soil microbial biomass and β-diversity. This was likely an indirect

467 process via the alteration of soil P content, C:P, N:P ratios, soil moisture, and pH. We believe

468 that bedrock may explain some of the inconsistencies surrounding previous studies of the

469 elevational patterns of soil microbial communities. We also anticipate that bedrock will modulate

470 the impacts of climate change on soil microbial communities.

471

Reference:

Antonelli, A., Kissling, W.D., Flantua, S.G.A., Bermúdez, M.A., Mulch, A., Muellner-Riehl, A.N., Kreft, H., Linder, H.P., Badgley, C., Fjeldså, J., Fritz, S.A., Rahbek, C., Herman, F., Hooghiemstra, H., Hoorn, C., 2018. Geological and climatic influences on mountain biodiversity. Nat. Geosci. 11, 718–725. https://doi.org/10.1038/s41561-018-0236-z

Augusto, L., Achat, D.L., Jonard, M., Vidal, D., Ringeval, B., 2017. Soil parent material—A major driver of plant nutrient limitations in terrestrial ecosystems. Glob. Change Biol. 23, 3808–3824. https://doi.org/10.1111/gcb.13691

Bahram, M., Hildebrand, F., Forslund, S.K., Anderson, J.L., Soudzilovskaia, N.A., Bodegom, P.M., Bengtsson-Palme, J., Anslan, S., Coelho, L.P., Harend, H., Huerta-Cepas, J., Medema, M.H., Maltz, M.R., Mundra, S., Olsson, P.A., Pent, M., Põlme, S., Sunagawa, S., Ryberg, M., Tedersoo, L., Bork, P., 2018. Structure and function of the global topsoil microbiome. Nature 560, 233–237. https://doi.org/10.1038/s41586-018-0386-6

Bayranvand, M., Akbarinia, M., Salehi Jouzani, G., Gharechahi, J., Kooch, Y., Baldrian, P., 2021. Composition of soil bacterial and fungal communities in relation to vegetation composition and soil characteristics along an altitudinal gradient. FEMS Microbiol. Ecol. 97, fiaa201. https://doi.org/10.1093/femsec/fiaa201

Bhople, P., Djukic, I., Keiblinger, K., Zehetner, F., Liu, D., Bierbaumer, M., Zechmeister-Boltenstern, S., Joergensen, R.G., Murugan, R., 2019. Variations in soil and microbial biomass C, N and fungal biomass ergosterol along elevation and depth gradients in Alpine ecosystems. Geoderma 345, 93–103. https://doi.org/10.1016/j.geoderma.2019.03.022

Bryant, J.A., Lamanna, C., Morlon, H., Kerkhoff, A.J., Enquist, B.J., Green, J.L., 2008. Microbes on mountainsides: Contrasting elevational patterns of bacterial and plant diversity. Proc. Natl. Acad. Sci. 105, 11505–11511. https://doi.org/10.1073/pnas.0801920105

Calderón-Sanou, I., Zinger, L., Hedde, M., Martinez-Almoyna, C., Saillard, A., Renaud, J., Gielly, L., Khedim, N., Lionnet, C., Ohlmann, M., Consortium, O., Münkemüller, T., Thuiller, W., 2022. Energy and physiological tolerance explain multi-trophic soil diversity in temperate mountains. Divers. Distrib. 28, 2549–2564. https://doi.org/10.1111/ddi.13529

Chen, J., Lewis, O.T., 2023. Limits to species distributions on tropical mountains shift from high temperature to competition as elevation increases. Ecol. Monogr. e1597. https://doi.org/10.1002/ecm.1597

Delgado-Baquerizo, M., Reich, P.B., Khachane, A.N., Campbell, C.D., Thomas, N., Freitag, T.E., Abu Al-Soud, W., Sørensen, S., Bardgett, R.D., Singh, B.K., 2017. It is elemental: soil nutrient stoichiometry drives bacterial diversity: C:N:P stoichiometry drives bacterial diversity. Environ. Microbiol. 19, 1176–1188. https://doi.org/10.1111/1462-2920.13642

Deng, H., Yu, Y.-J., Sun, J.-E., Zhang, J.-B., Cai, Z.-C., Guo, G.-X., Zhong, W.-H., 2015. Parent materials have stronger effects than land use types on microbial biomass, activity and diversity in red soil in subtropical China. Pedobiologia 58, 73–79. https://doi.org/10.1016/j.pedobi.2015.02.001

Fierer, N., 2017. Embracing the unknown: disentangling the complexities of the soil microbiome. Nat. Rev. Microbiol. 15, 579–590. https://doi.org/10.1038/nrmicro.2017.87

Fierer, N., McCain, C.M., Meir, P., Zimmermann, M., Rapp, J.M., Silman, M.R., Knight, R., 2011. Microbes do not follow the elevational diversity patterns of plants and animals. Ecology 92, 797–804. https://doi.org/10.1890/10-1170.1

Fierer, N., Strickland, M.S., Liptzin, D., Bradford, M.A., Cleveland, C.C., 2009. Global patterns in belowground communities. Ecol. Lett. 12, 1238–1249. https://doi.org/10.1111/j.1461-0248.2009.01360.x

Frostegård, A., Bååth, E., 1996. The use of phospholipid fatty acid analysis to estimate bacterial

and fungal biomass in soil. Biol. Fertil. Soils 22, 59–65.
https://doi.org/10.1007/BF00384433

Griffiths, R.I., Thomson, B.C., James, P., Bell, T., Bailey, M., Whiteley, A.S., 2011. The bacterial biogeography of British soils: Mapping soil bacteria. Environ. Microbiol. 13, 1642–1654. https://doi.org/10.1111/j.1462-2920.2011.02480.x

Hartmann, M., Six, J., 2022. Soil structure and microbiome functions in agroecosystems. Nat. Rev. Earth Environ. 4, 4–18. https://doi.org/10.1038/s43017-022-00366-w

He, X., Chu, C., Yang, Y., Shu, Z., Li, B., Hou, E., 2021. Bedrock and climate jointly control the phosphorus status of subtropical forests along two elevational gradients. CATENA 206, 105525. https://doi.org/10.1016/j.catena.2021.105525

He, X., Hou, E., Veen, G.F., Ellwood, M.D.F., Dijkstra, P., Sui, X., Zhang, S., Wen, D., Chu, C., 2020. Soil microbial biomass increases along elevational gradients in the tropics and subtropics but not elsewhere. Glob. Ecol. Biogeogr. 29, 345–354. https://doi.org/10.1111/geb.13017

He, X., Zeng, L., Zhu, G., Ellwood, M.D.F., Zhou, L., Huang, J., Wang, C., Li, W., Lin, D., Wei, P., Liu, S., Luo, M., Zhang, Y., Yang, Y., 2024. Parental material and climate jointly determine the biomass and diversity of soil microbial communities along an elevational gradient on a subtropical karst mountain. J. Biogeogr. https://doi.org/10.1111/jbi.14814

Hendershot, J.N., Read, Q.D., Henning, J.A., Sanders, N.J., Classen, A.T., 2017. Consistently inconsistent drivers of microbial diversity and abundance at macroecological scales. Ecology 98, 1757–1763. https://doi.org/10.1002/ecy.1829

Hu, A., Wang, Jianjun, Sun, H., Niu, B., Si, G., Wang, Jian, Yeh, C.-F., Zhu, X., Lu, X., Zhou, J., Yang, Y., Ren, M., Hu, Y., Dong, H., Zhang, G., 2020. Mountain biodiversity and ecosystem functions: interplay between geology and contemporary environments. ISME J. 14, 931–944. https://doi.org/10.1038/s41396-019-0574-x

Koranda, M., Kaiser, C., Fuchslueger, L., Kitzler, B., Sessitsch, A., Zechmeister-Boltenstern, S., Richter, A., 2014. Fungal and bacterial utilization of organic substrates depends on substrate complexity and N availability. FEMS Microbiol. Ecol. 87, 142–152. https://doi.org/10.1111/1574-6941.12214

Lang, F., Bauhus, J., Frossard, E., George, E., Kaiser, K., Kaupenjohann, M., Krüger, J., Matzner, E., Polle, A., Prietzel, J., Rennenberg, H., Wellbrock, N., 2016. Phosphorus in forest ecosystems: New insights from an ecosystem nutrition perspective. J. Plant Nutr. Soil Sci. 179, 129–135. https://doi.org/10.1002/jpln.201500541

Li, G., Xu, G., Shen, C., Tang, Y., Zhang, Y., Ma, K., 2016. Contrasting elevational diversity patterns for soil bacteria between two ecosystems divided by the treeline. Sci. China Life Sci. 59, 1177–1186. https://doi.org/10.1007/s11427-016-0072-6

Li, J., Shen, Z., Li, C., Kou, Y., Wang, Y., Tu, B., Zhang, S., Li, X., 2018. Stair-Step Pattern of Soil Bacterial Diversity Mainly Driven by pH and Vegetation Types Along the Elevational Gradients of Gongga Mountain, China. Front. Microbiol. 9, 569. https://doi.org/10.3389/fmicb.2018.00569

Li, X., Wang, T., Chang, S.X., Jiang, X., Song, Y., 2020. Biochar increases soil microbial biomass but has variable effects on microbial diversity: A meta-analysis. Sci. Total Environ. 749, 141593. https://doi.org/10.1016/j.scitotenv.2020.141593

Looby, C.I., Martin, P.H., 2020. Diversity and function of soil microbes on montane gradients: the state of knowledge in a changing world. FEMS Microbiol. Ecol. 96, fiaa122. https://doi.org/10.1093/femsec/fiaa122

Luan, L., Jiang, Y., Dini-Andreote, F., Crowther, T.W., Li, P., Bahram, M., Zheng, J., Xu, Q., Zhang, X.-X., Sun, B., 2023. Integrating pH into the metabolic theory of ecology to predict bacterial diversity in soil. Proc. Natl. Acad. Sci. 120, e2207832120. https://doi.org/10.1073/pnas.2207832120

Ma, L., Liu, L., Lu, Y., Chen, L., Zhang, Z., Zhang, H., Wang, X., Shu, L., Yang, Q., Song, Q.,

Peng, Q., Yu, Z., Zhang, J., 2022. When microclimates meet soil microbes: Temperature controls soil microbial diversity along an elevational gradient in subtropical forests. Soil Biol. Biochem. 166, 108566. https://doi.org/10.1016/j.soilbio.2022.108566

Ni, X., Liao, S., Wu, F., Groffman, P.M., 2022. Microbial biomass in forest soils under altered moisture conditions: A review. Soil Sci. Soc. Am. J. 86, 358–368. https://doi.org/10.1002/saj2.20344

Nottingham, A.T., Hicks, L.C., Ccahuana, A.J.Q., Salinas, N., Bååth, E., Meir, P., 2018. Nutrient limitations to bacterial and fungal growth during cellulose decomposition in tropical forest soils. Biol. Fertil. Soils 54, 219–228. https://doi.org/10.1007/s00374-017-1247-4

Peters, M.K., Hemp, A., Appelhans, T., Becker, J.N., Behler, C., Classen, A., Detsch, F., Ensslin, A., Ferger, S.W., Frederiksen, S.B., Gebert, F., Gerschlauer, F., Gütlein, A., Helbig-Bonitz, M., Hemp, C., Kindeketa, W.J., Kühnel, A., Mayr, A.V., Mwangomo, E., Ngereza, C., Njovu, H.K., Otte, I., Pabst, H., Renner, M., Röder, J., Rutten, G., Schellenberger Costa, D., Sierra-Cornejo, N., Vollstädt, M.G.R., Dulle, H.I., Eardley, C.D., Howell, K.M., Keller, A., Peters, R.S., Ssymank, A., Kakengi, V., Zhang, J., Bogner, C., Böhning-Gaese, K., Brandl, R., Hertel, D., Huwe, B., Kiese, R., Kleyer, M., Kuzyakov, Y., Nauss, T., Schleuning, M., Tschapka, M., Fischer, M., Steffan-Dewenter, I., 2019. Climate–land-use interactions shape tropical mountain biodiversity and ecosystem functions. Nature 568, 88–92. https://doi.org/10.1038/s41586-019-1048-z

Peters, M.K., Hemp, A., Appelhans, T., Behler, C., Classen, A., Detsch, F., Ensslin, A., Ferger, S.W., Frederiksen, S.B., Gebert, F., Haas, M., Helbig-Bonitz, M., Hemp, C., Kindeketa, W.J., Mwangomo, E., Ngereza, C., Otte, I., Röder, J., Rutten, G., Schellenberger Costa, D., Tardanico, J., Zancolli, G., Deckert, J., Eardley, C.D., Peters, R.S., Rödel, M.-O., Schleuning, M., Ssymank, A., Kakengi, V., Zhang, J., Böhning-Gaese, K., Brandl, R., Kalko, E.K.V., Kleyer, M., Nauss, T., Tschapka, M., Fischer, M., Steffan-Dewenter, I., 2016. Predictors of elevational biodiversity gradients change from single taxa to the multi-taxa community level. Nat. Commun. 7, 13736. https://doi.org/10.1038/ncomms13736

Philippot, L., Chenu, C., Kappler, A., Rillig, M.C., Fierer, N., 2023. The interplay between microbial communities and soil properties. Nat. Rev. Microbiol. https://doi.org/10.1038/s41579-023-00980-5

Porder, S., Ramachandran, S., 2013. The phosphorus concentration of common rocks—a potential driver of ecosystem P status. Plant Soil 367, 41–55. https://doi.org/10.1007/s11104-012-1490-2

Réjou-Méchain, M., Tanguy, A., Piponiot, C., Chave, J., Hérault, B., 2017. biomass : an r package for estimating above-ground biomass and its uncertainty in tropical forests. Methods Ecol. Evol. 8, 1163–1167. https://doi.org/10.1111/2041-210X.12753

Ren, C., Chen, J., Lu, X., Doughty, R., Zhao, F., Zhong, Z., Han, X., Yang, G., Feng, Y., Ren, G., 2018. Responses of soil total microbial biomass and community compositions to rainfall reductions. Soil Biol. Biochem. 116, 4–10. https://doi.org/10.1016/j.soilbio.2017.09.028

Rousk, J., Bååth, E., Brookes, P.C., Lauber, C.L., Lozupone, C., Caporaso, J.G., Knight, R., Fierer, N., 2010. Soil bacterial and fungal communities across a pH gradient in an arable soil. ISME J. 4, 1340–1351. https://doi.org/10.1038/ismej.2010.58

Seaton, F.M., George, P.B.L., Lebron, I., Jones, D.L., Creer, S., Robinson, D.A., 2020. Soil textural heterogeneity impacts bacterial but not fungal diversity. Soil Biol. Biochem. 144, 107766. https://doi.org/10.1016/j.soilbio.2020.107766

Sheng, R., Xu, H., Xing, X., Zhang, W., Hou, H., Qin, H., Liu, Y., Zhang, L., Fang, Y., Shen, J., Pernthaler, J., Wei, W., Zhu, B., 2023. The role of inherited characteristics from parent materials in shaping bacterial communities in agricultural soils. Geoderma 433, 116455. https://doi.org/10.1016/j.geoderma.2023.116455

624 Singh, D., Lee-Cruz, L., Kim, W.-S., Kerfahi, D., Chun, J.-H., Adams, J.M., 2014. Strong
625   elevational trends in soil bacterial community composition on Mt. Halla, South Korea.
626   Soil Biol. Biochem. 68, 140–149. https://doi.org/10.1016/j.soilbio.2013.09.027
627 Smith, L.C., Orgiazzi, A., Eisenhauer, N., Cesarz, S., Lochner, A., Jones, A., Bastida, F.,
628   Patoine, G., Reitz, T., Buscot, F., Rillig, M.C., Heintz-Buschart, A., Lehmann, A., Guerra,
629   C.A., Waring, B.G., 2021. Large-scale drivers of relationships between soil microbial
630   properties and organic carbon across Europe. Glob. Ecol. Biogeogr. 30, 2070–2083.
631   https://doi.org/10.1111/geb.13371
632 Spinola, D., Portes, R., Fedenko, J., Lybrand, R., Dere, A., Biles, F., Trainor, T., Bowden, M.E.,
633   D'Amore, D., 2022. Lithological controls on soil geochemistry and clay mineralogy
634   across Spodosols in the coastal temperate rainforest of southeast Alaska. Geoderma
635   428, 116211. https://doi.org/10.1016/j.geoderma.2022.116211
636 Sun, L., Xun, W., Huang, T., Zhang, G., Gao, J., Ran, W., Li, D., Shen, Q., Zhang, R., 2016.
637   Alteration of the soil bacterial community during parent material maturation driven by
638   different fertilization treatments. Soil Biol. Biochem. 96, 207–215.
639   https://doi.org/10.1016/j.soilbio.2016.02.011
640 Sundqvist, M.K., Sanders, N.J., Wardle, D.A., 2013. Community and Ecosystem Responses to
641   Elevational Gradients: Processes, Mechanisms, and Insights for Global Change. Annu.
642   Rev. Ecol. Evol. Syst. 44, 261–280. https://doi.org/10.1146/annurev-ecolsys-110512-
643   135750
644 Tripathi, B.M., Stegen, J.C., Kim, M., Dong, K., Adams, J.M., Lee, Y.K., 2018. Soil pH mediates
645   the balance between stochastic and deterministic assembly of bacteria. ISME J. 12,
646   1072–1083. https://doi.org/10.1038/s41396-018-0082-4
647 Tytgat, B., Verleyen, E., Sweetlove, M., D'hondt, S., Clercx, P., Van Ranst, E., Peeters, K.,
648   Roberts, S., Namsaraev, Z., Wilmotte, A., Vyverman, W., Willems, A., 2016. Bacterial
649   community composition in relation to bedrock type and macrobiota in soils from the Sør
650   Rondane Mountains, East Antarctica. FEMS Microbiol. Ecol. 92, fiw126.
651   https://doi.org/10.1093/femsec/fiw126
652 Wang, R., He, X., Zhang, Q., Li, B., Shu, Z., Chu, C., 2024. Inconsistent elevational patterns of
653   soil microbial biomass, diversity, and community structure on four elevational transects
654   from subtropical forests. Appl. Soil Ecol. 201, 105462.
655   https://doi.org/10.1016/j.apsoil.2024.105462
656 Weemstra, M., Peay, K.G., Davies, S.J., Mohamad, M., Itoh, A., Tan, S., Russo, S.E., 2020.
657   Lithological constraints on resource economies shape the mycorrhizal composition of a
658   Bornean rain forest. New Phytol. 228, 253–268. https://doi.org/10.1111/nph.16672
659 Xiao, D., He, X., Zhang, W., Cheng, M., Hu, P., Wang, K., 2022. Diazotroph and arbuscular
660   mycorrhizal fungal diversity and community composition responses to karst and non-
661   karst soils. Appl. Soil Ecol. 170, 104227. https://doi.org/10.1016/j.apsoil.2021.104227
662 Yu, K., Van Den Hoogen, J., Wang, Z., Averill, C., Routh, D., Smith, G.R., Drenovsky, R.E.,
663   Scow, K.M., Mo, F., Waldrop, M.P., Yang, Y., Tang, W., De Vries, F.T., Bardgett, R.D.,
664   Manning, P., Bastida, F., Baer, S.G., Bach, E.M., García, C., Wang, Q., Ma, L., Chen,
665   B., He, X., Teurlincx, S., Heijboer, A., Bradley, J.A., Crowther, T.W., 2022. The
666   biogeography of relative abundance of soil fungi versus bacteria in surface topsoil. Earth
667   Syst. Sci. Data 14, 4339–4350. https://doi.org/10.5194/essd-14-4339-2022
668 Zakavi, M., Askari, H., Shahrooei, M., 2022. Bacterial diversity changes in response to an
669   altitudinal gradient in arid and semi-arid regions and their effects on crops growth. Front.
670   Microbiol. 13, 984925. https://doi.org/10.3389/fmicb.2022.984925
671 Zeng, L., He, X., Zhu, G., Zhou, L., Luo, M., Yin, X., Long, Y., Dai, J., Ouyang, X., Yang, Y.,
672   2023. Bedrock and climate jointly control microbial necromass along a subtropical
673   elevational gradient. Appl. Soil Ecol. 189, 104902.
674   https://doi.org/10.1016/j.apsoil.2023.104902

675 Zhou, G., Peng, C., Li, Y., Liu, S., Zhang, Q., Tang, X., Liu, J., Yan, J., Zhang, D., Chu, G.,
676   2013. A climate change-induced threat to the ecological resilience of a subtropical
677   monsoon evergreen broad-leaved forest in Southern China. Glob. Change Biol. 19,
678   1197–1210. https://doi.org/10.1111/gcb.12128
679

680   **Table 1**. **Results of the Wilcoxon test to compare the mean values of soil microbial**

681   **biomass and α-diversities between two bedrock transects.** Significantly higher mean values

682   are in bold. Unit of biomass is ug g^{-1} soil.

Variable	Granite (Mean ± SD)	Slate (Mean ± SD)	*w*	*p*
Fungal biomass	**1.33** ± 0.54	1.09 ± 0.37	1267	0.040
Bacterial biomass	38.62 ± 14.2	42.95 ± 9.58	791	0.074
Bacteria to fungi ratio	30.79 ± 10.49	**42.28** ± 11.66	476	<0.001
Gram+ to Gram- ratio	**0.81** ± 0.08	0.72 ± 0.05	1634	<0.001
Bacterial Chao1	3036 ± 294	**3344** ± 349	520	<0.001
Bacterial Shannon	5.89 ± 0.2	5.95 ± 0.27	864	0.234
Bacterial inv-Simpson	**104** ± 29	82 ± 28	1413	0.001
Fungal Chao1	1237 ± 187	**1364** ± 209	695	0.010
Fungal Shannon	4.12 ± 0.48	4.03 ± 0.68	1060	0.706
Fungal inv-Simpson	18 ± 8	16 ± 9	1119	0.394

683

684

685 **Table 2. Effects of elevation and bedrock, and their interaction on the variations of soil**

686 **microbial communities' characters.** Numbers in the table are the standardized linear

687 regression coefficients.

	Elevation	Bedrock	Elevation×Bedrock	Adjusted R^2
Bacterial biomass	0.88***	0.36*	-1.01***	0.372
Fungal biomass	0.80***	-0.49*	-1.08***	0.373
B:F biomass ratio	0.19*	0.93***		0.231
G^+ to G^- biomass ratio	0.31***	-1.06***		0.384
Bacterial Chao1 index	0.11	0.87***		0.182
Bacterial Shannon index	0.04	0.26		0.001
Bacterial inverse Simpson	0.17	-0.71***		0.140
Fungal Chao1 index	0.28**	0.62**		0.151
Fungal Shannon index	0.09	-0.12		0.001
Fungal inverse Simpson	-0.15	-0.20		0.001

688 Stars next to the numbers indicate significance in the regression model: *, **, *** indicates

689 significance at the 95%, 99% and 99.9% level, respectively; no star means $p > 0.05$.

690

691

692 **Table 3 Summary of optimal model parameters for microbial biomass variables.** This table

693 presents the best-fit model results for microbial biomass variables, derived from an initial full

694 model that included mean annual temperature (MAT), soil organic carbon (C), phosphorus (P),

695 moisture, clay content, pH, carbon-to-nitrogen ratio (C:N), above-ground biomass (AGB), and

696 plant Shannon diversity (Plant H). Additionally, interactions between bedrock type and specific

697 environmental variables (soil P, moisture, pH, and MAT) were incorporated.

Microbial Variable	Predictors	Estimate	*p*-value	Adjusted R^2
Bacterial Biomass	Soil C	9.316	<0.001	0.625
	Soil C:N	-4.936	<0.001	
	Soil P	6.011	0.008	
	Clay	-2.065	0.070	
	MAT×Bedrock	4.294	0.022	
	Soil P×Bedrock	-11.818	<0.001	
Fungal Biomass	Soil C	0.267	<0.001	0.453
	Soil C:N	-0.216	<0.001	
	Soil P	-0.351	<0.001	
	Moisture×Bedrock	0.288	0.009	
	MAT×Bedrock	0.221	0.047	
Bacterial-to-Fungal Biomass ratio	Moisture	3.715	0.002	0.502
	Plant H	3.163	0.001	
	Soil P	6.042	<0.001	
	Moisture×Bedrock	-9.585	<0.001	
Gram$^+$ to Gram$^-$ bacteria biomass ratio	Clay	-0.015	0.046	0.710
	MAT	0.014	0.018	
	pH	-0.027	0.028	
	Soil P×Bedrock	0.060	0.020	

699 **Table 4 Summary of optimal model parameters for microbial community diversity index.**
700 This table presents the best-fit model results for microbial diversity index, derived from an initial
701 full model that included mean annual temperature (MAT), soil organic carbon (C), phosphorus
702 (P), moisture, clay content, pH, carbon-to-nitrogen ratio, above-ground biomass (AGB), and
703 plant Shannon diversity. Additionally, interactions between bedrock type and specific
704 environmental variables (soil P, moisture, pH, and MAT) were incorporated.

Microbial Variable	Predictors	Estimate	p-value	Adjusted R2
Bacterial Shannon index	Clay	0.068	0.008	0.271
	MAT	-0.098	<0.001	
	Moisture	-0.063	0.033	
	pH	0.075	0.004	
Bacterial inverse Simpson index	Soil C	9.249	0.013	0.202
	Soil P	-12.539	<0.001	
	Moisture×Bedrock	15.275	0.020	
Fungal Shannon index	Soil P	-0.608	0.000	0.383
	AGB	-0.155	0.019	
	Moisture×Bedrock	0.081	0.119	
	Soil P×Bedrock	1.145	<0.001	
Fungal inverse Simpson index	Moisture	4.086	<0.001	0.332
	Soil P	-6.853	0.001	
	Soil C	-3.039	0.045	
	pH×Bedrock	7.561	0.004	
	Soil P×Bedrock	16.332	<0.001	

705

Figure 1. Soil microbial biomass along elevational transects on granite and slate

bedrock. (a) soil bacterial biomass; (b) soil fungal biomass; (c) bacterial biomass to fungal

biomass ratios; (d) gram-positive to gram-negative bacterial biomass ratios. Solid and dashed

lines indicate significant ($p < 0.05$) and nonsignificant ($p > 0.05$) linear regression relationships,
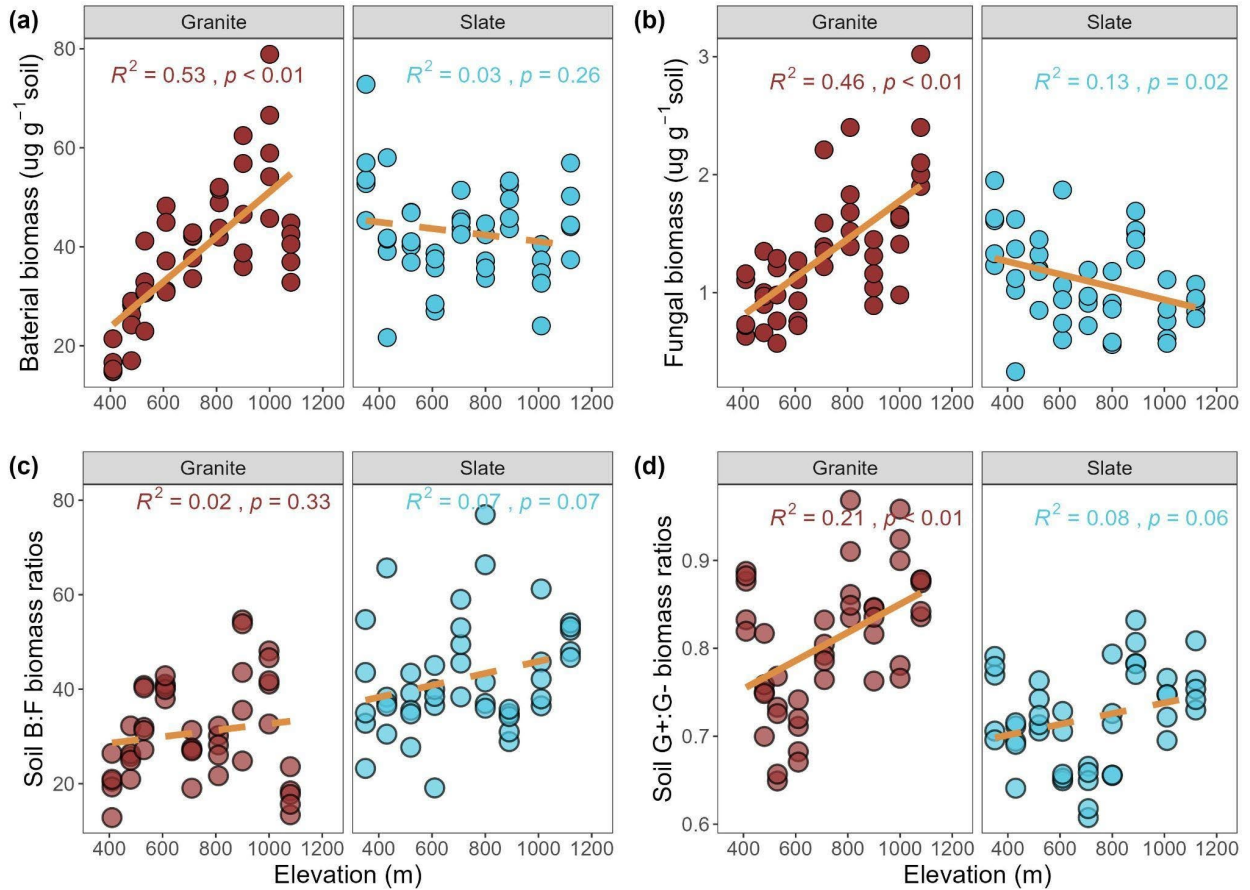
respectively.

713 **Figure 2. Elevational patterns of soil microbial community α-diversities**. (a and b) Shannon

714 and inverse Simpson diversity index of bacterial communities, respectively; (c and d) Shannon

715 and inverse Simpson diversity index of fungal communities, respectively. Dashed lines indicate

716 nonsignificant ($p > 0.05$) linear regression relationships.
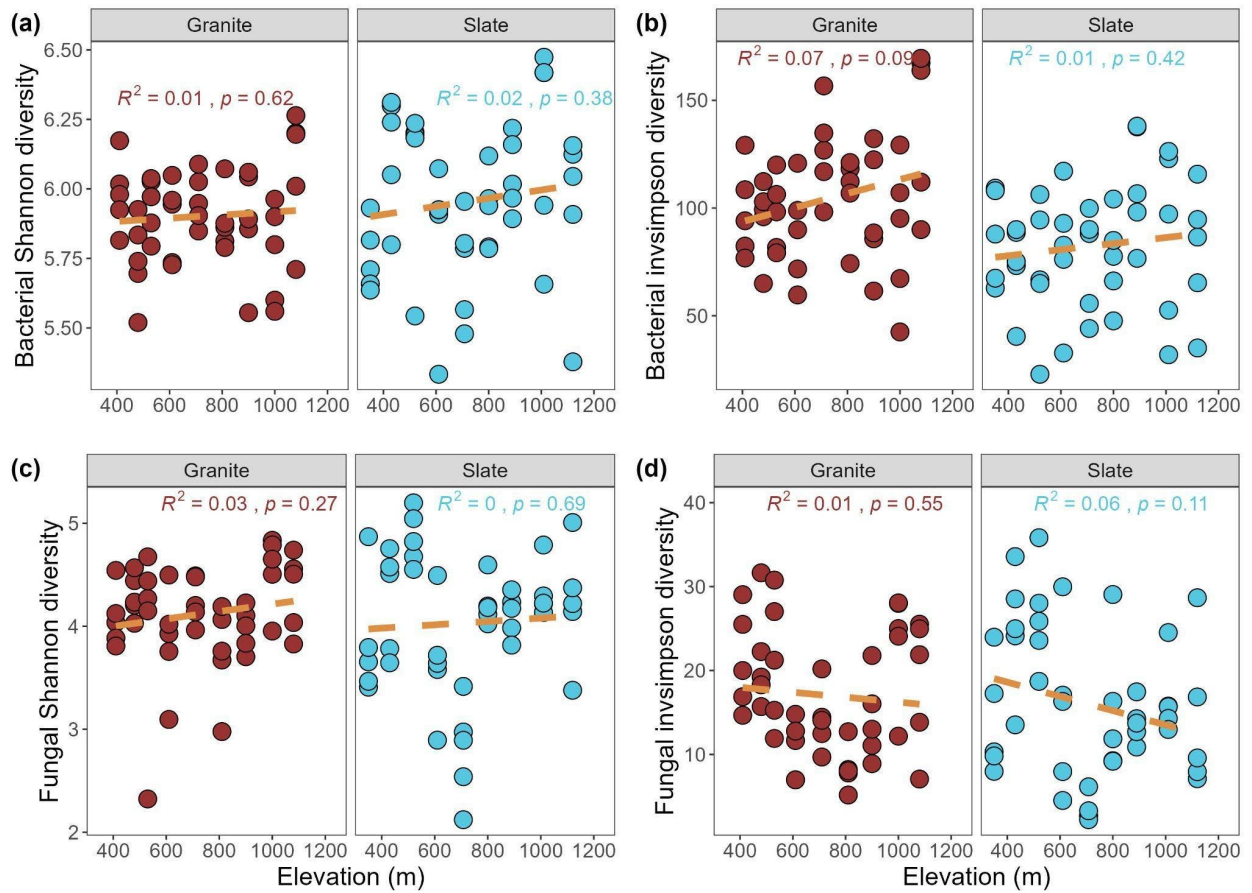
717

718

Figure 3. Distance-based redundancy analysis (db-RDA) of the relationship between predictor variables and the Bray–Curtis dissimilarity distance between microbial communities. Dots indicate individual samples; the arrow lengths and directions correspond to the variance explained by the individual variables. The figure shows the three most important variables to keep it concise. Figure S5 shows all the results for the variables' R^2.

Supplementary information of

726 Bedrock modulates the elevational patterns of soil microbial communities

727 Xianjin He1,2,*, Ruiqi Wang1,*, Daniel S. Goll2, Laurent Augusto3, Naoise Nunan4, M. D.

728 Farnon Ellwood5, Quanzhou Gao1, Junlong Huang6, Shenhua Qian6, Yonghua Zhang7, Zufei

729 Shu, Buhang Li1, Chengjin Chu1,#

730 1 State Key Laboratory of Biocontrol, School of Ecology, Shenzhen Campus of Sun Yat-sen

731 University, Shenzhen, 518033, China.

732 2 Laboratoire des Sciences du Climat et de l'Environnement, IPSL-LSCE, CEA/CNRS/UVSQ,

733 Orme des Merisiers, 91191, Gif sur Yvette, France.

734 3 ISPA, Bordeaux Sciences Agro, INRAE, 33140, Villenave d'Ornon, France.

735 17 Institute of Ecology and Environmental Sciences – Paris, Sorbonne Université, CNRS, IRD,

736 INRA, P7, UPEC, 4 place Jussieu, 75005 Paris, France.

737 18 Department of Soil and Environment, Swedish University of Agricultural Sciences, 75007

738 Uppsala, Sweden.

739 5 School of Environmental and Natural Sciences, Bangor University, Bangor, Gwynedd, LL57

740 2DG, United Kingdom.

741 6 Key Laboratory of the Three Gorges Reservoir Region's Eco-Environment, Ministry of

742 Education, Chongqing University, Chongqing, 400045, China.

743 7 College of Life and Environmental Science, Wenzhou University, Wenzhou, 325035, China.

744

745 * These authors contributed equally to this work.

746 #Correspondence to: chuchjin@mail.sysu.edu.cn.

747

748 **Table S1. Comparisons of climate, soil, and vegetation on contrasting bedrocks.**

Variable	Granite	Slate	w	p	Significance
MAT	21 ± 2.52	21.81 ± 3.47	875	0.268	ns
AGB	**20.46** ± 7.95	14.33 ± 3.86	1550	0.000	*
Plant Shannon	2.66 ± 0.49	**2.89** ± 0.37	675	0.006	*
Soil pH	4.41 ± 0.18	**4.67** ± 0.28	373	0.000	*
Soil moisture	0.18 ± 0.05	0.17 ± 0.03	950	0.616	ns
Bulk density	0.76 ± 0.21	**0.83** ± 0.15	723	0.019	*
SOC	81.49 ± 34.39	84.87 ± 27.09	880	0.288	ns
Soil TN	2.02 ± 0.88	**2.42** ± 0.63	661	0.004	*
Soil TP	0.23 ± 0.1	**0.49** ± 0.09	41	0.000	*
Soil C:N	**41.93** ± 12.09	34.76 ± 4.88	1469	0.000	*
Soil C:P	**397** ± 166	171 ± 40	1865	0.000	*
Soil N:P	**9.33** ± 2.64	4.9 ± 0.8	1868	0.000	*
Clay	40 ± 18.48	**64.78** ± 18.82	325	0.000	*
Silt	**28.02** ± 9.26	23.36 ± 8.69	1375	0.003	*
Sand	**31.67** ± 26.14	11.86 ± 21.32	1400	0.002	*
Slope direction	72 ± 63	51 ± 29	1038	0.843	ns

749

750

751

752 **Table S2.** Spearman correlation coefficients between soil microbial communities' characters

753 and environmental variables using all data from two transects. Significant coefficients ($p < 0.05$)

754 are in bold. B.Biomass: Bacterial biomass; F.Biomass: Fungal biomass; B.F.ratio: ratios of

755 bacterial to fungal biomass; G.G.ratio: ratios of gram positive to gram negative bacterial

756 biomass; Bacteria.H: Bacterial Shannon index; Bacteria.invs: Bacterial inverse Simpson index;

757 Fungi.H: Fungal Shannon index; Fungal.invs: Fungal inverse Simpson index.

	MAT	pH	Moisture	Clay	AGB	Plant.H	SOC	Soil.P	C:N	C:P	N:P
All											
B.Biomass	**-0.24**	-0.13	0.21	0.15	**-0.37**	-0.01	**0.56**	**0.38**	-0.10	-0.04	0.01
F.Biomass	-0.15	-0.06	0.05	-0.06	-0.20	-0.10	0.17	-0.17	0.01	**0.23**	**0.30**
B.F.ratio	-0.13	-0.03	**0.21**	**0.32**	-0.19	0.12	**0.33**	**0.63**	**-0.26**	**-0.41**	**-0.42**
G.G.ratio	**-0.29**	**-0.32**	-0.07	**-0.37**	-0.12	**-0.51**	**0.29**	**-0.40**	**0.38**	**0.67**	**0.69**
Bacteria.H	-0.16	**0.27**	-0.05	0.19	-0.15	-0.07	-0.07	0.06	0.03	-0.08	-0.11
Bacteria.invs	-0.13	**-0.23**	-0.09	-0.17	0.09	**-0.21**	0.07	**-0.35**	**0.34**	**0.41**	**0.38**
Fungi.H	**-0.28**	0.06	0.15	-0.02	-0.25	-0.03	-0.02	0.10	-0.11	-0.07	-0.09
Fungi.invs	-0.04	0.15	**0.27**	-0.05	-0.11	-0.05	-0.20	-0.04	-0.12	-0.10	-0.12

758

759 **Table S3. Spearman correlation coefficients between soil microbial communities'**

760 **characters and environmental variables on granite and slate, respectively.** Significant

761 coefficients ($p < 0.05$) are in bold. B.Biomass: Bacterial biomass; F.Biomass: Fungal biomass;

762 B.F.ratio: ratios of bacterial to fungal biomass; G.G.ratio: ratios of gram positive to gram

763 negative bacterial biomass; Bacteria.H: Bacterial Shannon index; Bacteria.invs: Bacterial

764 inverse Simpson index; Fungi.H: Fungal Shannon index; Fungal.invs: Fungal inverse Simpson

765 index.

	MAT	pH	Moisture	Clay	AGB	Plant.H	SOC	Soil.P	C:N	C:P	N:P
Granite											
B.Biomass	**-0.37**	**-0.31**	0.24	0.27	**-0.38**	0.09	**0.76**	**0.66**	-0.23	0.01	0.23
F.Biomass	**-0.36**	0.01	**-0.33**	0.00	**-0.53**	-0.16	**0.43**	0.13	-0.06	0.25	**0.51**
B.F.ratio	-0.07	**-0.41**	**0.72**	**0.40**	0.15	**0.32**	**0.38**	**0.71**	**-0.35**	**-0.40**	**-0.39**
G.G.ratio	-0.19	0.06	**-0.35**	**-0.34**	**-0.52**	**-0.53**	**0.35**	-0.17	0.26	**0.55**	**0.65**
Bacteria.H	-0.08	**0.38**	-0.23	0.14	0.02	-0.26	-0.04	-0.12	0.23	0.17	0.16
Bacteria.invs	-0.15	0.09	**-0.30**	-0.03	-0.20	-0.09	0.12	-0.20	0.24	**0.34**	**0.37**
Fungi.H	**-0.30**	-0.03	0.19	**-0.30**	-0.22	-0.21	0.11	0.07	-0.07	-0.08	-0.07
Fungi.invs	-0.17	-0.01	0.26	**-0.45**	-0.15	-0.44	-0.04	-0.02	0.05	-0.08	-0.21
Slate											
B.Biomass	-0.07	-0.21	0.05	0.01	-0.15	-0.08	0.20	0.09	0.12	0.22	0.24
F.Biomass	0.12	0.20	**0.42**	0.18	-0.07	0.25	-0.16	-0.13	-0.12	-0.10	-0.04
B.F.ratio	-0.08	**-0.33**	**-0.51**	-0.17	0.03	**-0.40**	**0.30**	0.20	0.19	0.23	0.17
G.G.ratio	**-0.45**	-0.09	0.26	0.19	**-0.43**	-0.10	**0.36**	**0.43**	0.14	0.20	0.20
Bacteria.H	-0.26	**0.32**	0.00	0.11	-0.08	0.22	-0.13	-0.02	-0.06	-0.10	-0.17
Bacteria.invs	-0.09	-0.18	0.21	0.07	0.02	-0.09	0.12	-0.05	0.21	0.23	0.11
Fungi.H	**-0.36**	**0.33**	0.02	0.10	**-0.41**	**0.34**	-0.16	**0.34**	-0.22	**-0.34**	**-0.37**
Fungi.invs	-0.05	**0.45**	0.19	0.25	-0.24	**0.46**	**-0.37**	0.12	**-0.32**	**-0.47**	**-0.46**

766

767 **Figure S1. Distribution of sampling sites along two subtropical elevational transects.** (a)
768 Location of the sampling sites within East Asia, indicated by a red square; (b) Distribution of
769 sites along the two transects, where red dots represent granite sites and blue dots represent
770 slate sites. Elevations are marked by numbers near each dot. The base map is a color-coded
771 DEM derived from SRTM 90m data.

772

773
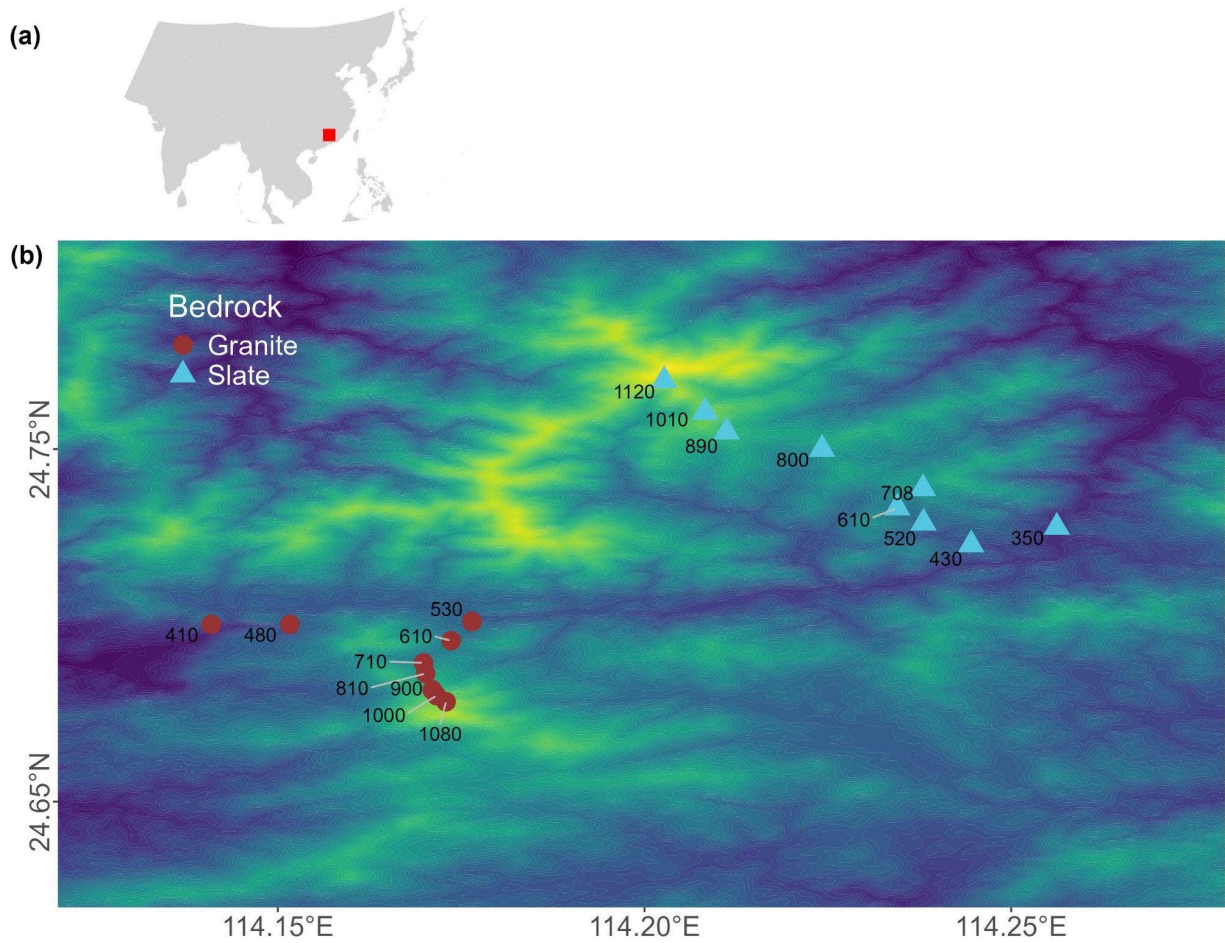
Figure S2. Elevational patterns of soil temperature, moisture, and vegetation characteristics on granite and slate bedrock. (a) Mean annual soil temperature; (b) Mean annual soil moisture; (c) Plant diversity, measured by the Shannon index; (d) Above-ground biomass. Solid and dashed lines indicate significant ($p < 0.05$) and nonsignificant ($p > 0.05$) linear regression relationships, respectively.

779
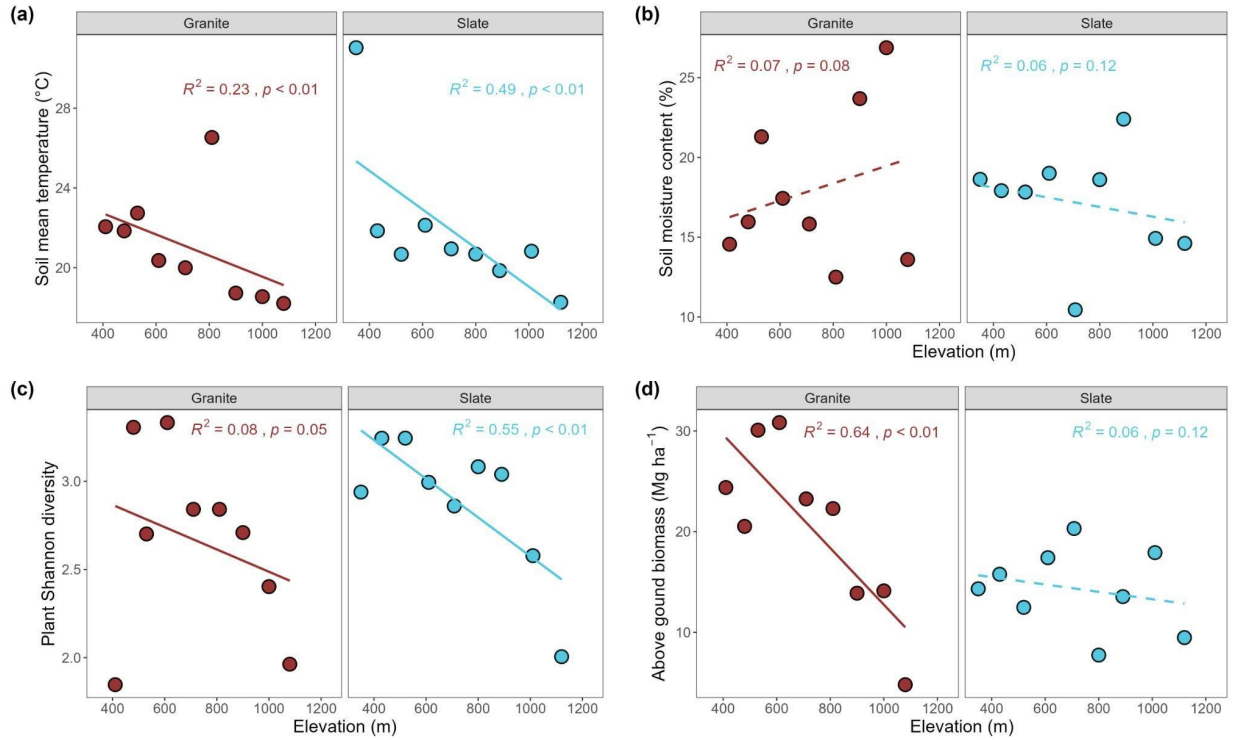
Figure S3. Elevational patterns of soil physical-chemical properties on granite and slate bedrock. (A) soil organic carbon concentration; (B) soil total phosphorus concentration; (C) soil clay content; (D) soil silt content; (E) soil pH; (F) soil moisture. Solid and dashed lines indicate significant ($p < 0.05$) and non-significant ($p > 0.05$) linear regression relationships, respectively.
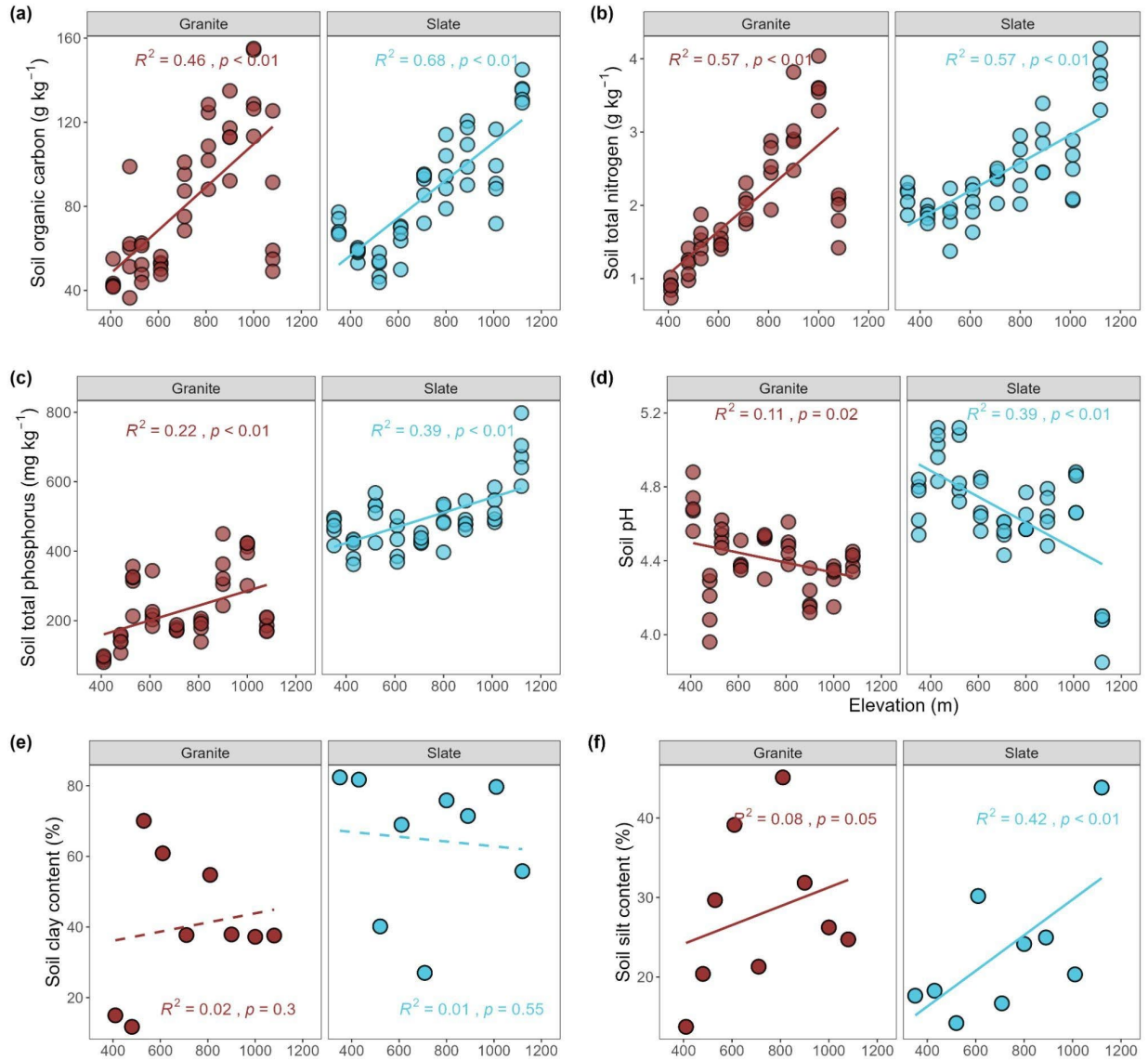
784

785

786 **Figure S4. Principal Component Analysis (PCA) of environmental variables vary along**

787 **two elevational transects on granite and slate bedrocks.**

PCA of environmental variables with bedrock type and elevation

788

789
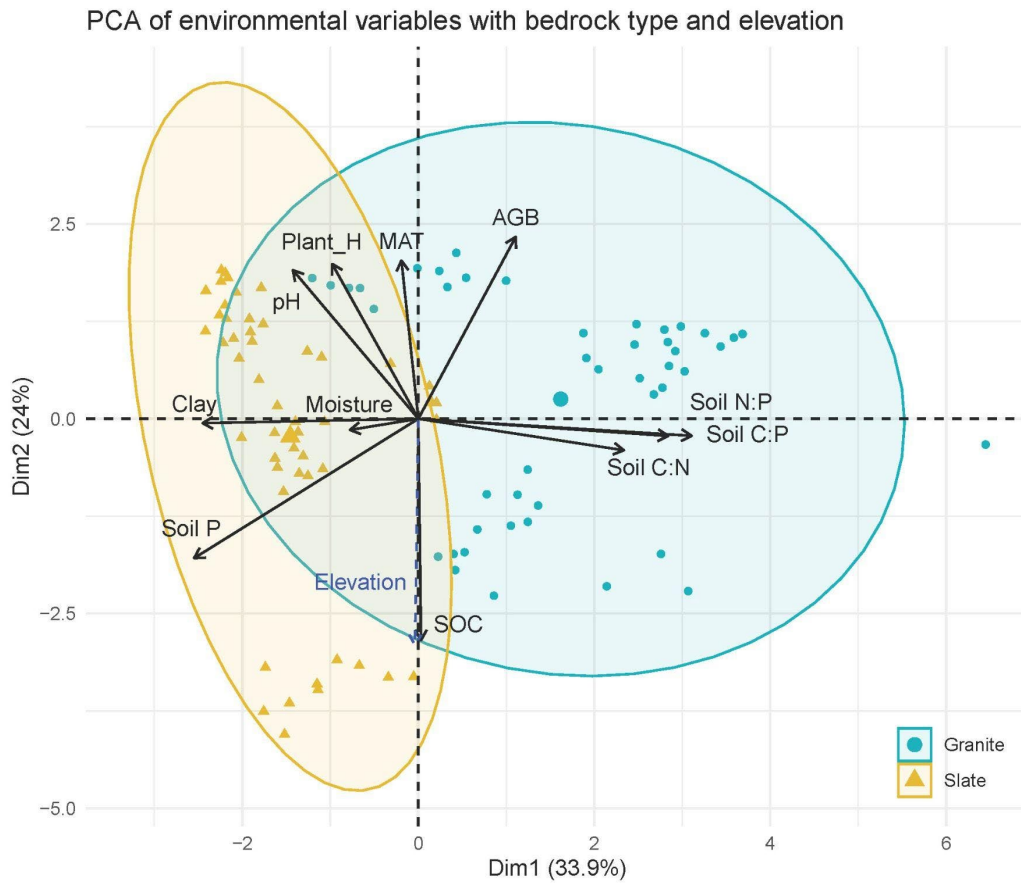
Figure S5. Variables' R^2 in the redundancy analysis (RDA) in Figure 3 in the main text. R^2
indicates the proportion of variation of soil microbial communities explained by the variables,
respectively. Star next to a bar indicates that it is statistically significant ($p < 0.05$).
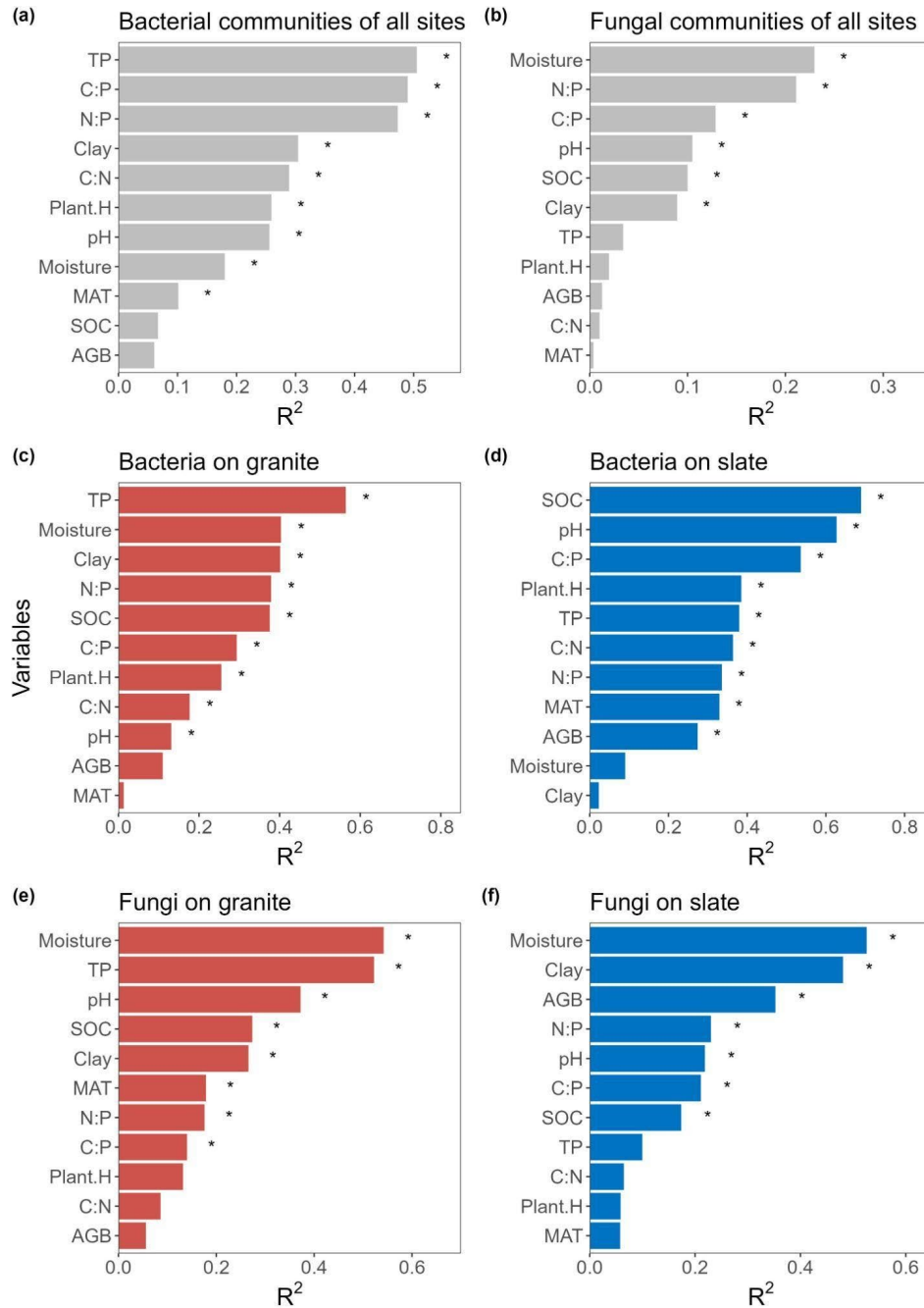
795 **Figure S6. Effects of bedrock on microbial community assembly processes.** (a–b) Fit of

796 the neutral community model to bacterial communities on granite and slate, respectively. (c–d)

797 Fit of the neutral community model to fungal communities on granite and slate, respectively.

798 Black dots indicate the best fit to the model (± 95% confidence intervals); R^2 values indicate

799 level of neutral community model prediction accuracy and Nm indicates estimated migration

800 volume of samples. "R^2" represented overall goodness of fit of the NCM, with higher values

801 indicating that the improved fit was the result of stochastic processes; "N" represented microbial

802 metacommunity size (number of OTUs); "m" represented migration rate of microbes, with

803 smaller values indicating less diffusion limitation.

804